ELSEVIER

Journal of Chromatography A, 927 (2001) 111–120

JOURNAL OF CHROMATOGRAPHY A

www.elsevier.com/locate/chroma

Behavior of *n*-alkanes on poly(oxyethylene) capillary columns Evaluation of interfacial effects

F.R. González[a,b,*], R.C. Castells[b,c], A.M. Nardillo[b,c]

[a]*Instituto de Química Física Rocasolano, CSIC, Serrano 119, 28006 Madrid, Spain*

[b]*Div. Química Analítica, Fac. de Ciencias Exactas, Universidad Nacional de La Plata, 47 y 115,1900 La Plata, Argentina*

[c]*CIDEPINT, 52 y 121, 1900 La Plata, Argentina*

Received 13 April 2001; received in revised form 26 June 2001; accepted 26 June 2001

Abstract

The solvation behavior of *n*-alkanes on poly(oxyethylene) was studied employing capillary gas chromatography. Interfacial effects were discriminated and evaluated through the analysis of retention data from six commercial fused-silica capillary columns, having film thicknesses of 0.15–5 μm. Expressions for the mixed retention mechanism in capillary columns were deduced from assumptions of a general character. Partition coefficients were determined for the *n*-alkanes up to 28 carbon atoms, at temperatures ranging from 40 to 240°C. In agreement with other authors, it was observed that interfacial phenomena contribute poorly to the chromatographic retention, being negligible over 140°C for homologues with less than 16 carbons.

Keywords: Capillary columns; Poly(oxyethylene) stationary phases; Stationary phases, GC; Partition coefficients; Alkanes

1. Introduction

The partition–adsorption mixed mechanism of retention emerged as a matter of study at the early stage of development of gas–liquid chromatography (GLC). The literature on this theme has been reviewed by several authors, e.g. Martire [1], Berezkin [2,3], Conder and Young [4] and Poole et al. [5]. More recently, Poole et al. [6] and Berezkin [7] have reviewed the latest advances in this topic. It has repeatedly been remarked that systems of polar solvents with non-polar solutes and vice versa, exacerbate the effects of the interfacial phenomena. An extensive study on the incidence of such effects in the GLC retention of packed columns has been carried out [5]. The authors concluded that partition is generally the principal process governing retention in the usual chromatographic temperature range. Interfacial effects were shown to be relevant for the non-polar alkane solutes on the polar poly(oxyethylene) stationary phases. In packed columns of Carbowax 20M, *n*-alkanes are mainly retained by partition at 120°C, but adsorption becomes significant toward 80°C [8,9]. Orav et al. [10] investigated the retention on stainless steel capillary columns coated with Carbowax 20M. They found that the *n*-alkanes display the strongest adsorption effects, compared to the other solutes studied. Employing glass capillary columns of Superox-20M, Fernández-Sánchez et al. [11] did not detect any dependence of the specific retention volume on the film thickness of the col-

*Corresponding author.

E-mail address: rex@quimica.unlp.edu.ar (F.R. González).

0021-9673/01/$ – see front matter
PII: S0021-9673(01)01077-9

umns, for solutes with molar masses lower than that of dodecane.

The low ratio of liquid volume to interfacial area in capillary columns, namely the small film thickness, d_f, of the coated stationary phase ($V_L/A_i = d_f \sim 10^{-5}$ cm), makes the assessment of interfacial effects unavoidable for the *n*-alkane–poly(oxyethylene) system. On the other hand, the simple geometry of wall-coated capillaries has great advantages in facilitating the control of the geometric variables. Furthermore, the control of the chemical properties of the solid surface is simpler for highly pure silica capillaries.

The chromatographic performance of high average molecular-mass poly(oxyethylene), Superox 2 or 4, has drawn much attention with regard to its thermal stability [12,13]. The thermal stability is further improved through polymer cross-linking. Notable differences are observed in the relative retention between bonded and cross-linked phases [14]. Soft crosslinking has the effect of lowering the melting interval of the polymer and reducing its crystalline fraction [15]. Using other stationary phases, Berezkin and Korolev concluded that the impact of adsorption increases with polymer crosslinking [16]. Surowiec and Rayss [17] found that, below its melting point (~60°C), Carbowax 20M exhibits partition as the leading factor in retention. According to Sandra et al. [15], when an important crystalline fraction has been grown in the stationary phase, the solutes eluting between 40 and 60°C are separated solely by the adsorption mechanism.

Both crosslinking and the increment of the crystalline fraction have the effect of increasing the density, and thus diminishing the free volume in the dense phase. As an immediate consequence, the excluded volume effects become increasingly important. The augmented work of cavity formation will then be responsible for reducing the absolute value of the free energy of solute transfer from the gas to the bulk polymer. In this way, the influence of partition would be diminished.

Due to the good wetting characteristics of Superox and Carbowax on glass and fused silica [13,15] in contrast with hydrocarbons, a greater affinity of poly(oxyethylene) to the column solid wall than that of alkane solutes is an aspect to be considered in these systems.

Our aim is to study the retention behavior of *n*-alkanes on silica capillary columns coated with poly(oxyethylene). The high numeral density of monomer units in this polymer, in conjunction with the relatively high ratio of solute/solvent monomeric volumes, should magnify the features currently controlled by repulsive forces, i.e. by the excluded volume effects. Hence, the general trends for the behavior of some retention parameters can be highlighted through the comparison with observations made on other systems [18,19].

2. General

The extant anisotropy at the interfaces introduces border effects or perturbations to the 'structural' properties of an isotropic liquid that is in contact with a gas and solid phases. The perturbation propagates into the liquid lattice a certain distance, *d*, perpendicular to the interface plane, fading gradually until the bulk average properties of this phase are met. If the liquid is a neutral amorphous polymer, the longest range of this propagation takes place through the backbone of the chains, due to the existence of correlation between bond directions in a chain molecule [20]. Average values of *d* of several angstroms are expected for poly(oxyethylene). Considering that in the stationary phase of a capillary column the polymer film thickness, d_f, may be of the order of 10^3 Å, we must admit the relative importance of the perturbation depth *d*. This parameter only depends on the structural properties of the polymer chain and its environment. Therefore, it is a relevant thermodynamic parameter from a molecular point of view[1].

We shall not make any assumption here on the processes actually taking place at the interfaces. However, as an illustration, let us consider a hypo-

[1]The perturbation depth, *d*, can thus be defined unambiguously in terms of molecular parameters from current statistical mechanics of chain molecules. In continuum thermodynamics the definition of an equivalent theoretical entity is usual. This requires settling conventions on the location of the Gibbs dividing surface; for a discussion on this topic and IUPAC definitions on this issue see, for example, Ref. [21].

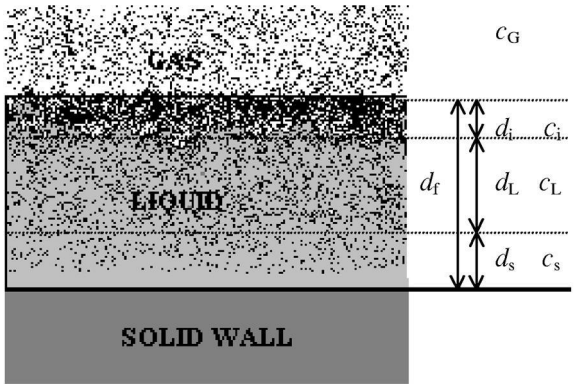

Fig. 1. Scheme illustrating different regions in the liquid, or subphases, that are considered should be discriminated in the partition of the solute on a polymeric film coating the wall of a capillary column.

thetical case for the effects of interfacial phenomena on the equilibrium distribution of a solute in a capillary column (Fig. 1). Accumulation of solute at the gas–liquid (G–L) and depletion at the solid–liquid (S–L) interphases, with respect to the bulk liquid, are assumed in this arbitrarily chosen example. The effect at the G–L interface should be the consequence of a decrease in the interfacial free energy per unit area (the surface tension) in the liquid solution due to the accumulation of solute [22]. Let d_i be the distance necessary to travel, from the G–L surface into the bulk liquid, for finding the constant average properties of the latter. Since a concentration gradient is expected due to the continuous variation of the properties in the perturbed liquid lattice, we can then define an average concentration of solute, C_i, at the Gibbs region so delimited by the perturbation depth d_i (i.e. the interphase or subphase):

$$C_i \equiv \frac{N_i}{A_i d_i} \tag{1}$$

N_i is the number of solute molecules in this subphase and A_i is the G–L interfacial area. Concentrations may be expressed either as mass/molar concentrations, or like in Eq. (1) as the number density of molecules. Similarly, the existence of a subphase of depth d_s and average concentration C_s can be postulated for the S–L interface. In Fig. 1 we have assumed that depletion of solute molecules takes place at this interfacial region. If the solute has less affinity towards the solid wall than the solvent, we must also consider that polymer–solid interactions will affect the properties of the liquid lattice hosting the solute. Through attractive interactions, the pattern of the solid structure will induce a certain order into the adjacent liquid along the perturbation depth d_s. Excluded volume effects may be increased locally, so yielding an average concentration C_s in this region that will be lower than the concentration C_L found in the bulk liquid.

So generally speaking, three regions in the stationary phase coating of thickness d_f are distinguished: (a) the region at the G–L interface of perturbation depth, d_i, where an average solute concentration C_i can be defined; (b) a region at the S–L interface of perturbation depth d_s, where an average concentration C_s can be defined; (c) the region of depth d_L and concentration C_L, where the properties of the bulk solution are met. While the distances d_i and d_s are thermodynamic quantities dependent only on the structural characteristics of the interacting system, d_L is not. The latter depends also on the film thickness of the column, which is fixed by the column manufacturer:

$$d_L = d_f - (d_i + d_s) \tag{2}$$

From the molecular standpoint, the relevant thermodynamic constant describing solvation of the solute into the bulk solvent is the distribution coefficient K [23]:

$$K = \frac{C_L}{C_G} \tag{3}$$

where $C_G \equiv N_G/V_G$ is the numeral density of solute molecules in the gas phase. Since the average excess concentration of solute in the interfacial regions is referred with respect to the bulk liquid, the involved thermodynamic constants are written in the following way:

$$e_i \equiv K_i - 1 = \frac{C_i - C_L}{C_L} \quad e_s \equiv K_s - 1 = \frac{C_s - C_L}{C_L} \tag{4}$$

$\ln K_i$ and $\ln K_s$ define average reduced free energies of transfer for the solute molecule from the bulk solvent into the respective interfacial subphases. The

excesses settled in Eq. (4) will be referred to, respectively, as the G–L and the S–L 'excess'. This denomination will be preserved no matter what is the sign of the difference, namely if e corresponds to accumulation or to depletion with respect to the bulk solution.

According to the current theory, the motion of a chromatographic band is described by the differential equation:

$$\frac{dz}{dt} = uR \quad R = \frac{N_G}{N_G + N_L} \tag{5}$$

The retardation factor, R, is the probability of finding the solute molecule in the gas phase, u is the local velocity of the carrier gas, and dz/dt is the local migration rate of the band center of mass. Integration of Eq. (5) leads to the well known retention equation, assuming a symmetrical band:

$$t_R = t_M(1 + k) \tag{6}$$

t_R denotes the solute retention time and t_M the gas hold-up time. The retention factor is $k \equiv N_L/N_G$. The total number of solute molecules in the stationary phase, N_L, accounts for the effects of the interfaces. Then, a mass balance should be done, so that all contributions are included. Using the definition of Eq. (1), the equivalent for the S–L subphase and Eq. (2):

$$N_L = C_i A d_i + C_s A d_s + C_L A\,[d_f - (d_i + d_s)] \tag{7}$$

We have assumed that the G–L and S–L interfacial areas are approximately equal, $A \equiv A_i \cong A_s$, a condition satisfied if the internal diameter of the capillary complies with $d_c \gg d_f$ [see Eq. (11)]. Considering that the volume of gas phase with this condition is $V_G = Ad_c/4$, a relationship between the retention factor and the film thickness is derived by using Eqs. (3), (4) and (7):

$$k\frac{d_c}{4} = K(e_i d_i + e_s d_s) + K d_f. \tag{8}$$

An equivalent expression is obtained by dividing both sides by d_f:

$$K_{ap} = K + K\,(e_i d_i + e_s d_s)\frac{1}{d_f} \tag{9}$$

where we have defined the apparent distribution coefficient $K_{ap} \equiv k\beta$. The phase ratio of the column is $\beta = V_G/V_L = d_c/4d_f$. According to Eq. (6), K_{ap} is directly obtainable through chromatographic measurement on a given column: $K_{ap} = [(t_R/t_M) - 1]\beta$. In the same way as k, K_{ap} includes all contributions to retention, partition and interfacial excesses and consequently depends on d_f:

$$K_{ap} = K_{ap}(T, d_f)$$

Eqs. (8) and (9) are both linear expressions, the ordinates being experimentally measurable quantities, while the slopes and intercepts are unknown parameters. Their physical significance is immediate, albeit more straightforwardly revealed in Eq. (9). This states that when the extension of interfacial area tends to be small with respect to the volume of liquid, the measured apparent coefficients tend to the value of the distribution coefficient at the bulk solution:

$$d_f^{-1} = A/V_L \to 0, K_{ap} \to K$$

Eqs. (8) and (9) are the ones to be applied for the analysis of the experimental results. Although physically they express the same, we shall employ both, because the errors on d_c and d_f are computed differently in each. Therefore, the discrepancy of results arising from their application will reflect the impact of those errors.

In contrast with the Martin–Berezkin classical linear equation [2,24–27], for deriving Eqs. (8) and (9) there was no need to formulate any hypothesis on the nature of the mechanisms of the interfacial excesses; or whether these mechanisms are independent or interdependent, or about the concentration regime and the extent of coverage of active sites on the solid wall. Eqs. (8) and (9) simply express a mass balance and state that the relevant thermodynamic parameters are the perturbation depths and the ratio of solute molecules average numeral densities for all subphases [23]. The latter are the perturbed liquid fractions at the interfaces and the unperturbed bulk liquid. There are no other constraints, beside those just enumerated and the geometric approximations. Even where d would be arbitrarily taken as greater than the real distance at which the interfacial perturbation has been damped to be negligible, the equations are still valid. Over-

estimating d will be compensated for by the corresponding reduction of e. The inverse is not valid, because something would be missing in the balance. Knowledge of the exact values of d_i and d_s and their associated excesses, are irrelevant for our purposes, considering that we can only perceive their combined effect through chromatographic measurement. Hence, we shall refer to $(e_i d_i + e_s d_s)$ as the 'net interfacial excess'. This is the unique parameter of interfacial effects accessible to our present experimental approach.

3. Experimental

Six columns, with the same origin, covering most of the commercially available range for d_f, were employed in this study. The specifications provided by the manufacturer are given in Table 1. These specifications correspond to ambient T. The temperature dependence of column phase ratio, originated in a different thermal expansion of the stationary phase polymer and the solid silica wall, was calculated according to:

$$\frac{\beta(T)}{\beta(T_o)} = \frac{d_c(T)\, d_f(T_o)}{d_f(T)\, d_c(T_o)} = e^{\frac{(\alpha_{SiO_2} - \alpha_{PEG})}{3}(T - T_o)}$$

$$\alpha \equiv \frac{1}{V}\left(\frac{\partial V}{\partial T}\right)_p \qquad (10)$$

T_o is any reference temperature. Eq. (10) assumes volume thermal expansion coefficients of column materials, α, to be constant in the temperature interval. The thermal expansion coefficient of silica is $\alpha_{SiO_2} = 1.6 \cdot 10^{-6}\ K^{-1}$ [28] and for poly(oxyethylene) approximately is $\alpha_{PEG} = 9.5 \cdot 10^{-4}\ K^{-1}$ [29]. Due to the greater thermal expansion of the liquid compared with the solid wall, an increment of 32 K translates into a decrease of 1% in the value of β.

In a capillary column the ratio of G–L to S–L interfacial areas departs from unity according to:

$$\frac{A_i}{A_s} = 1 - \frac{2d_f}{d_c} = 1 - \frac{1}{2\beta} \qquad (11)$$

The application of Eqs. (8) and (9) is justified if: (a) this departure from unity is small and (b) A_i/A_s is kept practically constant. Condition (b) arises from the fact that $e_i d_i$ and $e_s d_s$ contribute differently to K_{ap} and may even have different signs. Although (a) is satisfied, we see in Table 1 that increments for d_f are not accompanied with increments for d_c in the same proportion, in order to preserve d_f/d_c constant. However, the errors so generated are much lower than the errors in the specification of d_f.

The experimental conditions for obtaining the data presented here are the same as those described in Refs. [18,19]. Determination of gas hold-up, t_M, was carried out through the regression method of the *n*-alkanes, as in the cited papers.

4. Results and discussion

4.1. Behavior of methane

The *n*-alkanes regression method for gas hold-up determination simply consists in the application, under constant conditions, of general retention Eq. (6) to a homologous series [30]. For a mixed retention mechanism Eq. (6) should be written as:

$$t_R(n) = t_M + e^{\ln(t_M/\beta) + \ln K_{ap}(n)} \qquad (12)$$

In the second term, only one parameter independent

Table 1
Column specifications; the columns are AT-wax from AllTech (USA)

Column	Length L (m)	Bore diameter d_c (μm)	Film thickness d_f (μm)	Nominal phase ratio β
1	30	250	0.15	417
2	30	250	0.25	250
3	30	250	0.50	125
4	10	540	1.2	112
5	30	530	2.5	53
6	30	530	5.0	26.5

of the number of carbon atoms n can be determined through least-square regression of $t_R(n)$ data. Then (t_M/β) must be combined with the intercept A of function $\ln K_{ap}(n)$ as a single parameter A' ($A' = \ln (t_M/\beta) + A$). Through the analysis of the retention data it is found that only non-linear $\ln K_{ap}(n)$ test functions provide very accurate curve fits to $t_R(n)$. For this reason, the same mathematical form of the regression equation for pure partition [18] was used: $t_R(n) = t_M + \exp [A' + B(n-1) + \ln (1 - Cn^2)]$. Of course, the physical interpretation of the parameters now differs.

For columns with $\beta > 125$ there are no significant discrepancies between calculated t_M and the retention time of methane $t_R(CH_4)$, as can be seen in the examples given in Table 2. Fig. 2 shows the apparent partition coefficients of methane obtained from retention on the two columns with lowest β values, the only ones allowing significant differences between $t_R(CH_4)$ and t_M. Despite the great experimental errors, we see most $K_{ap}(CH_4)$ data lying in a band between 0.3 and 0.5, following a weak temperature dependence. Based on the small value of $K_{ap}(CH_4)$ and its rather small dependence on temperature, we must conclude that the adsorption of methane should have a minor impact on retention. Therefore, $K(CH_4)$ should be the major contribution to $K_{ap}(CH_4)$. The observed behavior of the apparent coefficient can be explained through the great impact of the work of cavity formation on the partition of methane, giving place to $K(CH_4) < 1$ at moderate temperatures. This is one immediate consequence of the high numeral density of solvent monomers in the stationary-phase and the relatively high volume ratio for solute/solvent monomers [18,30]. These values of K are in the same order as those determined, through static methods, in other low free-volume dense phases.

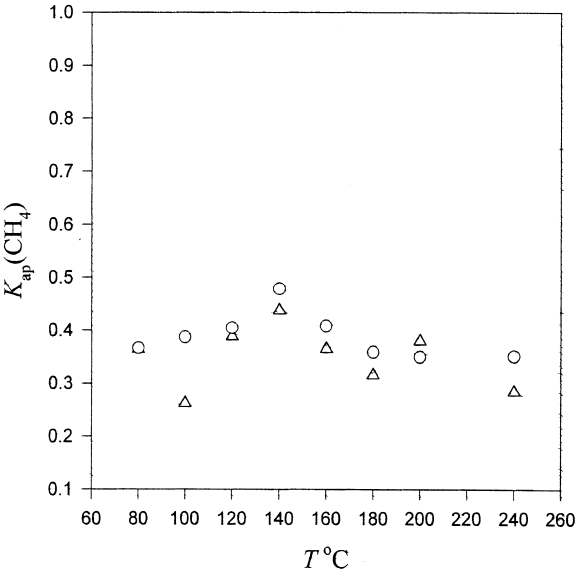

Fig. 2. Apparent distribution coefficients of methane determined at different temperatures. These were calculated from retention data on columns 1 and 2 (lowest available β).

One example is $K(CH_4)$ measured by several authors in n-hexadecane, reported to be in the range 0.45–0.51 [31]. In this system the ratio of monomeric volumes (solute/solvent) is high. Other examples are $K(CH_4)$ measured on poly(dimethylsiloxane) elastomers, which are densely cross-linked rubbers. These are found to vary around 0.45 at ambient temperature [32,33].

4.2. Evaluation of interfacial effects for n-alkanes

The retention data of the studied alkanes were utilized for least-square regression analysis applying Eqs. (8) and (9). Fig. 3 illustrates graphically the

Table 2
Comparison of t_M calculated by the n-alkanes regression method[a] with the retention time of methane in the different columns

T (°C)	$\beta = 26.5$		$\beta = 53$		$\beta = 125$		$\beta = 250$		$\beta = 417$	
	$t_R(CH_4)$	t_M	$t_R(CH_4)$	t_M	$t_R(CH_4)$	t_M	$t_R(CH_4)$	t_M	$t_R(CH_4)$	t_M
40	0.937	0.911	1.627	1.618	0.902	0.898	1.743	1.739	0.954	0.953
80	1.016	1.002	1.775	1.762	0.978	0.975	0.963	0.960	1.039	1.038
120	1.101	1.084	1.919	1.903	1.062	1.057	1.031	1.029	1.139	1.138
160	1.173	1.155	1.043	1.034	1.137	1.134	1.103	1.101	1.214	1.212
200	1.140	1.122	1.109	1.101	1.212	1.206	1.173	1.171	1.292	1.289

[a] The retentions of peaks with widths at half the height $w_h > 0.1$ min were not included in the regressions [18].

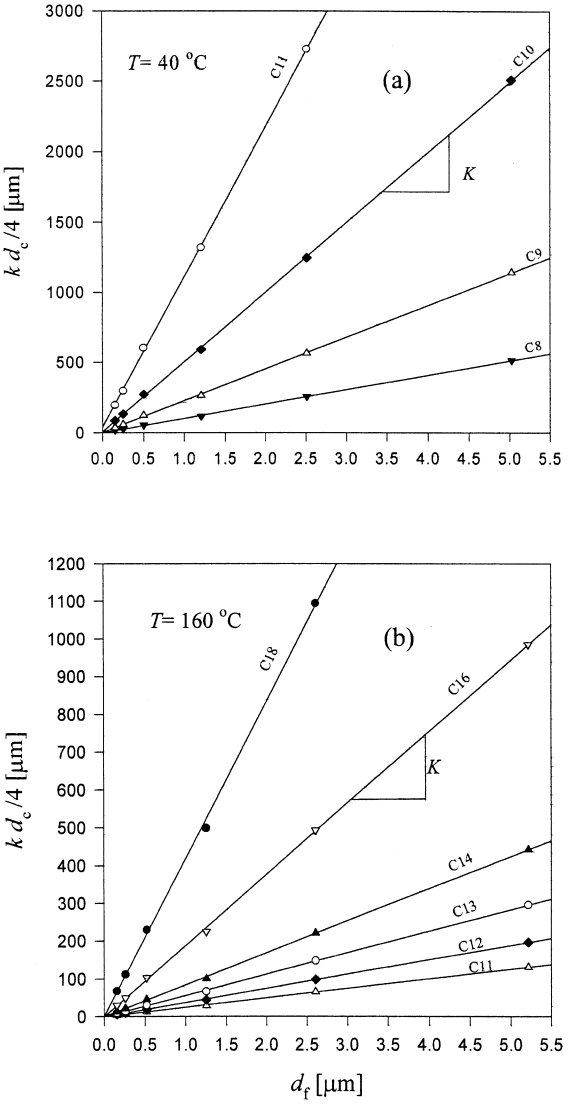

Fig. 3. Representation of retention data in accordance with Eq. (8). (a) At 40°C significant ordinates at the origin can be observed. (b) At 160°C the intercepts at the origin are not significant.

application of Eq. (8) at two temperatures. In these graphs, the slope yields the partition coefficient K and the intercepts render the product $K(e_i d_i + e_s d_s)$. Only at the low T and for the higher homologues, can intercepts lying out of the origin that overcome the random plot dispersion be graphically discriminated. For the high T these intercepts are not significant, being lower than their standard error of determination even for homologues with n as high as 16. Fig. 4 represents Eq. (9). Now K is the ordinate at the origin and $K(e_i d_i + e_s d_s)$ is the slope. We then have a closer graphical approach to the magnitude of experimental errors affecting the estimation of the latter. Typically, discrepancies between both regression analysis are $<0.5\%$ for K and $<20\%$ for the net excess $(e_i d_i + e_s d_s)$. Fig. 5 presents values of $(e_i d_i +$

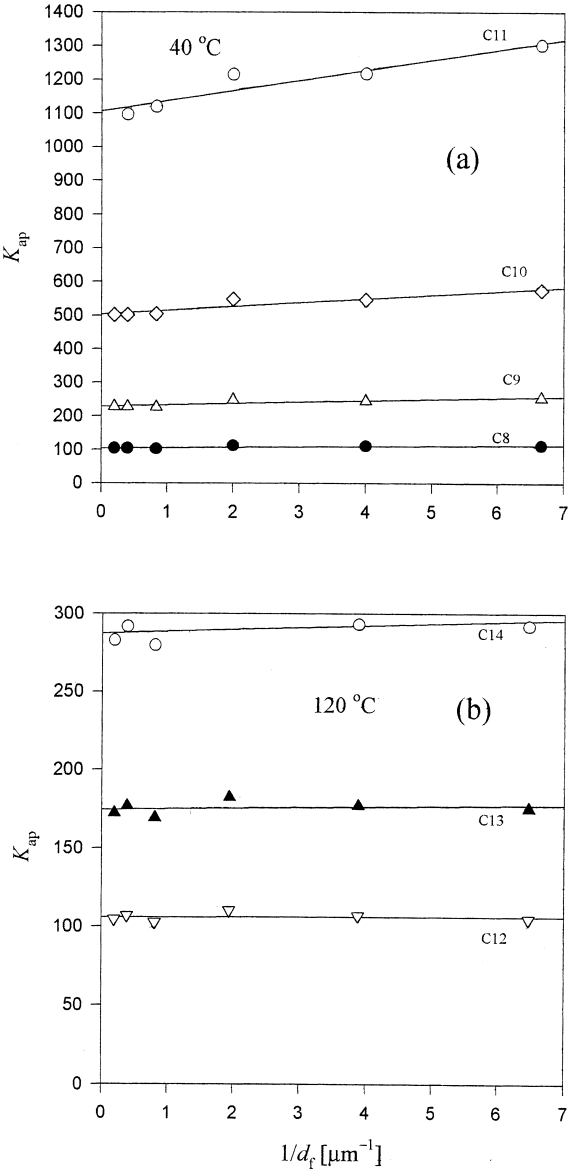

Fig. 4. Representation of retention data in accordance with Eq. (9). (a) At 40°C important slopes are observed. (b) At 120°C only for the higher homologues is the slope perceptible.

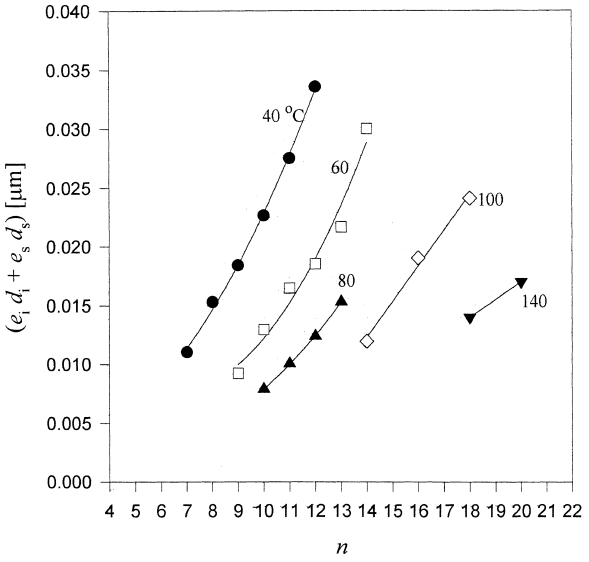

Fig. 5. Net interfacial excess plotted as function of *n*, at different temperatures.

$e_s d_s$) found to be statistically significant. The net excess is positive in all cases, no significant negative excesses were detected. This fact does not rule out that negative excesses could be possible at the L–S subphase, $e_s d_s$ could be negative but lower than $e_i d_i$ in absolute value.

According to Eq. (9) the quotient of the net excess and d_f yields the error committed when using K_{ap} in place of the rigorously determined K:

$$\text{error\%} \equiv \left(\frac{K_{ap} - K}{K}\right) \cdot 100 = \left(\frac{e_i d_i + e_s d_s}{d_f}\right) \cdot 100 \quad (13)$$

For example, we see in Fig. 5 that for C_{14} at 100°C this error approximately is 1% in a column with $d_f = 1$ μm, while it is obviously 10% in a column with $d_f = 0.1$ μm.

4.3. Partition coefficients of n-alkanes

Table 3 presents the values of K obtained through the regression of K_{ap} data to Eq. (9). These results are shown graphically in Fig. 6. There are no perceptible changes in the behavior of $K(n)$ below the polymer melting interval, i.e. for 40°C. We must admit that no major changes in the structural properties of the dense phase take place in the transition. Temperature variation of monomer numeral density

Table 3
ln K of *n*-alkanes at different temperatures, determined using Eq. (9)

n	*T* (°C)									
	40	60	80	100	120	140	160	180	200	240
5	2.223	1.900	1.560							
6	3.041	2.579	2.205	1.877				0.969		
7	3.831	3.307	2.846	2.454				1.347		
8	4.630	4.020	3.481	3.011	2.644		1.998	1.724	1.506	
9	5.423	4.726	4.115	3.583	3.143	2.757	2.403	2.089	1.838	
10	6.211	5.427	4.742	4.159	3.659	3.219	2.816	2.481	2.186	1.674
11	6.988	6.126	5.368	4.719	4.161	3.667	3.218	2.845	2.524	1.950
12	7.783	6.831	5.991	5.275	4.662	4.119	3.624	3.201	2.859	2.260
13	8.576	7.530	6.610	5.832	5.162	4.565	4.028	3.571	3.177	2.530
14		8.203	7.239	6.377	5.659	5.014	4.434	3.938	3.492	
16					6.649	5.903	5.237	4.666	4.149	3.344
18				8.548	7.597		6.031	5.385	4.806	3.881
20						7.607	6.774	6.081	5.454	4.414
22							7.551	6.785	6.093	4.941
24							8.317	7.462	6.709	5.467
26								8.134	7.333	5.991
28									7.897	6.511
30										7.020

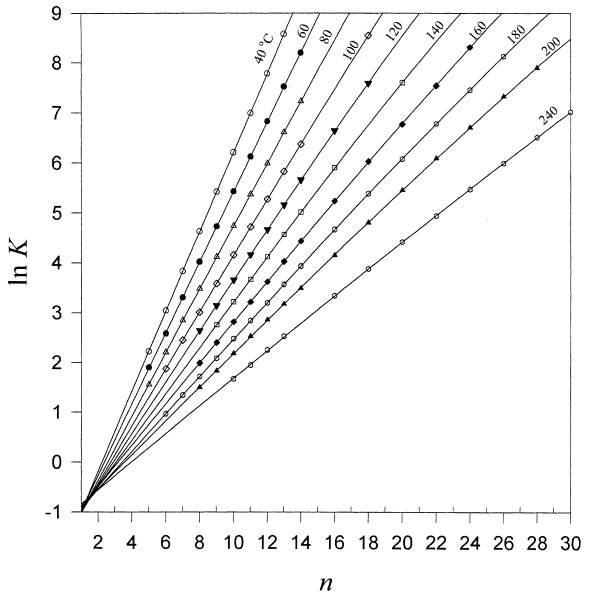

Fig. 6. ln $K(n)$ functions at different temperatures. Symbols are the experimental data and filled lines are the regression equation $\ln K(n)=A+B\ (n-1)+\ln\ (1-C\ n^2)$. The intercepts of these functions for $n=1$ have the same order of ln K of methane and also reveal a weak temperature dependence.

and the radial distribution-function would preserve the behavior of the liquid, provided a rapid cooling from this state.

Fig. 6 shows that extrapolation of ln $K(n)$ to $n=1$ yields intercepts that have the same order of ln $K_{ap}(CH_4)$ (~ -0.9). The intercepts also present a weak variation with T. The described behavior resembles that observed in a poly(dimethylsiloxane) solvent, where extrapolated curves of n-alkanes to $n=1$ yield intercepts which have the same order of ln $K(CH_4)$ at $T>120$°C [18]. On a physical basis, we should not expect in general that the solution properties of n-alkanes, extrapolated to one methylene unit, be similar to that of the CH_4 molecule. However, since these intercepts generally present ln $K\leq 0$, the dominance of the work of cavity formation in the solvation process for a hypothetically isolated $-CH_2-$ and CH_4 makes them similar. The Van der Waals radii are similar for these two entities.

Table 4 compares our results with the values of K reported by Poole et al. [6]. The latter are partition coefficients determined on Carbowax 20M, employing packed columns. The average discrepancy for the whole table is $\delta\%=1.2\%$. The discrepancies are not randomly distributed, they follow a systematic pattern. The main structural difference between the employed phases is that AT-wax is softly cross-linked. This can not only lead to a proportional difference in $K(n)$, but to a slightly different temperature dependence [19].

5. Conclusions

Retention data of n-alkanes on fused-silica columns of poly(oxyethylene) were analyzed making no consideration other than assuming that the existence of interfaces originate solute excesses over finite extensions of the liquid phase and minor geometric approximations. The results presented here corroborate commonly accepted statements relative to the range of temperatures where the retention is seriously affected by interfacial phenomena. For the level of accuracy of the reported results, a thumb rule can be stated. Over 140°C and for n lower than 16, contri-

Table 4
Comparison of ln K for AT-wax, of data reported here and Carbowax 20M, reported in Ref. [6][a]

n	81.2°C			101.2°C			121.2°C			141.2°C		
	[b]	Ref. [6]	$\delta\%$	[b]	Ref. [6]	$\delta\%$	[b]	Ref. [6]	$\delta\%$	[b]	Ref. [6]	$\delta\%$
11	5.349	5.275	−1.4				4.154	4.129	−0.6			
12	5.970	5.904	−1.1	5.263	5.183	−1.5	4.651	4.651	0	4.115	4.145	0.73
13	6.580	6.523	−0.87	5.814	5.736	−1.3	5.147	5.158	0.2	4.563	4.621	1.3
14				6.360	6.288	−1.1	5.640	5.664	0.4	5.011	5.183	3.4
16							6.635	6.668	0.5	5.892	6.123	3.9

[a] Data of Ref. [6] was obtained on packed columns.
[b] Data reported in Table 3 were interpolated to the indicated temperatures using a polynomial of order 5.

butions of interfacial excesses to K_{ap} are below the error of determination.

Acknowledgements

This work was sponsored by Consejo Nacional de Investigaciones Científicas y Técnicas de La República Argentina (CONICET) and by Agencia Nacional de Promoción Científica y Tecnológica, contract BID 802/OC-AR. F.R.G. is holder of an external fellowship from CONICET, at Instituto de Química-Física Rocasolano, CSIC, Madrid, Spain.

References

[1] D.E. Martire, in: J.H. Purnell (Ed.), Progress in Gas Chromatography, Wiley, New York, 1968.
[2] V.G. Berezkin, J. Chromatogr. 159 (1978) 359.
[3] V.G. Berezkin, Gas–Liquid–Solid Chromatography, Marcel Dekker, New York, 1991.
[4] J.R. Conder, C.L. Young, Physicochemical Measurement by Gas Chromatography, Wiley, New York, 1979.
[5] S. K Poole, T.O. Kollie, C.F. Poole, J. Chromatogr. A 664 (1994) 229.
[6] C.F. Poole, Q. Li, W. Kiridena, W.W. Koziol, J. Chromatogr. A 898 (2000) 211.
[7] V.G. Berezkin, Adv. Chromatogr. 40 (2000) 599.
[8] B.R. Kersten, C.F. Poole, J. Chromatogr. 399 (1987) 1.
[9] C.F. Poole, T.O. Kollie, S.K. Poole, Chromatographia 34 (1992) 281.
[10] A. Orav, K. Kuningas, T. Kailas, E. Koplimets, S. Rang, J. Chromatogr. A 659 (1994) 143.
[11] E. Fernández-Sánchez, A. Fernández-Torres, J.A. García-Domínguez, E. López de Blas, J. Chromatogr. A 655 (1993) 11.
[12] M. Verzele, P. Sandra, J. Chromatogr. 158 (1978) 111.
[13] R.F. Arrendale, R.F. Severson, O.T. Chortyk, J. Chromatogr. 208 (1981) 209.
[14] J.K.G. Kramer, R.C. Fouchard, K.J. Jenkins, J. Chromatogr. Sci. 23 (1985) 54.
[15] P. Sandra, F. David, R.A. Turner, H.M. Mc Nair, A.D. Brownstein, J. Chromatogr. 411 (1989) 63.
[16] V.G. Berezkin, A.A. Korolev, Chromatographia 20 (1985) 482.
[17] K. Surowiec, J. Rayss, Chromatographia 37 (1993) 444.
[18] F.R. González, J. Chromatogr. A 873 (2000) 209.
[19] F.R. González, L.G. Gagliardi, J. Chromatogr. A 879 (2000) 157.
[20] J.P. Flory, Statistical Mechanics of Chain Molecules, Interscience, New York, 1969.
[21] K.S. Yun, C. Zhu, J.F. Parcher, Anal. Chem. 67 (1995) 613.
[22] F.C. Goodrich, The thermodynamics of fluid interfaces, in: Surface and Colloid Science, Vol. I, Wiley-Interscience, New York, 1969.
[23] A. Ben Naim, Solvation Thermodynamics, Plenum Press, New York, 1987.
[24] R.L. Martin, Anal. Chem. 33 (1961) 347.
[25] R.L. Martin, Anal. Chem. 35 (1963) 116.
[26] J.R. Conder, D.C. Locke, J.H. Purnell, J. Phys. Chem. 73 (1969) 700.
[27] H.L. Liao, D.E. Martire, Anal. Chem. 44 (1972) 493.
[28] Catalog, Polymicro Technologies, AZ, 1994.
[29] B.R. Kersten, S.K. Poole, C.F. Poole, J. Chromatogr. 468 (1989) 235.
[30] F.R. González, J. Chromatogr. A 832 (1999) 165.
[31] P.J. Hesse, R. Battino, P. Scharlin, E. Wilhelm, J. Chem. Eng. Data 41 (1996) 195.
[32] M.G. De Angelis, J. Pol. Sci. B 37 (1999) 3011.
[33] V.M. Shah, B. Hardy, S.A. Stern, J. Pol. Sci. B 24 (1986) 2033.